International Journal of
Automotive Manufacturing and Materials (IJAMM)

Article

Simulation of Vibration Characteristics of the Front MacPherson Suspension of a Sightseeing Vehicle

Deli Li [1,2], Ling Rong [1], Nairui Mao [1], Yuanmei Song [1,*], Ruquan Liang [1,*], and Jinwen You [1]

[1] School of Mechanical & Vehicle Engineering, Linyi University, Linyi 276000, China
[2] College of Engineering Science and Technology, Shanghai Ocean University, Shanghai 201306, China
* Correspondence: ymsong321@163.com (Y.S.); liangruquan@lyu.edu.cn (R.L.)
Received: 07 July 2024; Revised: 24 September 2024; Accepted: 10 October 2024; Published: 16 October 2024

Abstract: This paper utilizes MATLAB/Simulink to simulate the vibration characteristics of the quarter-front MacPherson independent suspension of a sightseeing vehicle under random road conditions. Key performance indicators, including vehicle body acceleration, suspension deflection, and tire dynamic load, are comprehensively investigated. Focusing on the influence of suspension stiffness and damping on ride comfort and the service life of the vehicle, we conduct a comparative analysis by gradually changing the stiffness and damping parameters from the original design. Comparison of the simulation results across different stiffness and damping settings provides a profound understanding of how these parameters significantly affect the ride comfort and service life of the sightseeing vehicle. These findings not only provide valuable guidance for the design and manufacturing of customized optimized suspension systems for sightseeing vehicles, but also enrich the content and broaden the scope of current research.

Keywords: sightseeing vehicle suspension; vibration characteristics; service life; comfort; Simulink simulation

1. Introduction

With the rapid development of the modern automotive industry, the performance requirements for vehicles have become increasingly stringent. Among these, the suspension system, as a crucial factor affecting the ride comfort and stability of a vehicle, has always been a focus of attention for researchers and engineers. The primary function of the suspension system is to improve ride comfort and vehicle control [1], and it not only directly relates to the riding experience of passengers, but also involves various issues such as vehicle handling stability, safety, and road adaptability [2]. Therefore, in-depth research and optimization of the suspension system are of significant importance for improving the overall performance of a vehicle.

On the theoretical research front, researchers have established various mathematical models and simulation systems to predict and analyze the performance of suspension systems. For instance, the use of hierarchical control for electronically controlled air suspension ride height systems based on variable structure and fuzzy control theory has achieved active control of vehicle suspension systems, aiming to enhance the comfort and safety of vehicles [3]. Additionally, with the continuous development of computer technology and numerical simulation methods, finite element analysis [4] and multi-body dynamics simulation [5] have become essential tools for studying suspension systems. For example, Karthikeyan et al. [6] conducted a non-linear finite element analysis on hyperelastic materials in automotive suspension systems, focusing on durability and stress concentration under various loading conditions, while Sadegh Yarmohammadisatri et al. [7] developed a robust multi-body dynamics model to evaluate the effects of suspension geometry on steering mechanisms and vehicle behavior under probabilistic uncertainties.

In parallel, sightseeing vehicles, designed specifically for tourism purposes, present distinct challenges for suspension systems due to their unique operational requirements. These vehicles typically travel at lower speeds, carry larger numbers of passengers, and operate on diverse road surfaces such as city streets, scenic routes, and uneven rural roads. Therefore, their suspension systems must possess enhanced vibration absorption capabilities to maintain a high level of ride comfort and safety. To address these specific demands, an increasing number of researchers are utilizing simulation technology to study and optimize the vibration characteristics of sightseeing vehicles. For instance, Dong Mingfeng [8] built a road excitation model and a two-degree-of-freedom vehicle suspension model in MATLAB/Simulink for simulation analysis, comparing the effects of active and passive suspensions on indicators such as body acceleration, suspension deflection, and wheel dynamic load.

Based on previous research, this paper continues to explore the impact of suspension stiffness and damping on vibration characteristics using simulation methods.

2. The Dynamic Model for the Suspension System

In the MATLAB/Simulink environment, a simulation model of the suspension system of a sightseeing vehicle can be established. By inputting different vehicle parameters, the vibration response of the suspension can be simulated under random road surface of grade B. This simulation analysis can not only help to gain a deeper understanding of the performance characteristics of the suspension system, but also provide important basis for the optimization design of the suspension. In addition, MATLAB/Simulink also provides rich data processing and visualization tools, which can intuitively observe and analyze the vibration characteristics of suspension systems, such as vibration frequency, amplitude, etc.

The commonly used vehicle models include: (1) a 1/4 vehicle two degree of freedom model, considering the vertical motion of the sprung mass and the unsprung mass; (2) 1/2 vehicle four degree of freedom model, considering the vertical motion of the mass under the single side front and rear springs, as well as the vertical and pitch motion of the mass on the spring; (3) A seven degree of freedom model for the entire vehicle, considering the vertical motion of the mass under the front and rear springs on both sides, as well as the vertical motion, pitch motion, and roll motion of the mass on the springs. This research adopts a 1/4 vehicle two degree of freedom model. This model is widely applied in suspension system research and is considered a simplified yet effective tool for studying vertical dynamics. the quarter-car model not only plays a key role in suspension analysis but is also widely used in the design and validation of vehicle body control systems, particularly in the study of vertical dynamic control [9]. It considers the vertical motion of both the unsprung mass and the sprung mass, as shown in Figure 1. The corresponding parameters and symbols are listed in Table 1.

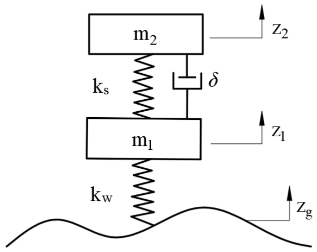

Figure 1. 1/4 Passive suspension model with two degrees of freedom for a vehicle.

Table 1. Table of model parameter meanings.

Symbol	Significance	Symbol	Significance
m_1	Unsprung mass	δ	Suspension damping coefficient
m_2	Sprung mass	Z_g	Vertical ground displacement (road input)
k_w	Tire stiffness	Z_1	Vertical displacement of unspring loaded mass
k_s	Suspension stiffness	Z_2	Vertical displacement of spring-loaded mass

The vast majority of suspension systems widely used in road vehicles by all major manufacturers are passive [10], and this simulation is based on the Texas Pastor new energy electric sightseeing vehicle. The following targeted suspension design and optimization will be conducted referring to the specific needs and characteristics of the model. The relevant parameters are detailed in Table 2.

Table 2. Parameters of Pastor new energy electric sightseeing car.

Physical Quantity Name	Parameter
name	8-seater iron shell sightseeing bus
electrical machinery	72 V/4 kw AC
battery	6 maintenance-free 12 V/100 AH power batteries
range	≤ 100 km
curb weight	1100 kg
External dimensions	4500 × 1560 ×2050 mm
wheelbase	2250 mm
Trackwidth (front/rear)	1320/1370 mm
Maximum driving speed	≤ 30 km/h
Steering	Rack and pinion steering gear
powertrain	Continuously variable transmission system, central lever shift
brake system	Front disc and rear drum four-wheel hydraulic brakes, handbrake parking

The suspension mass distribution coefficient (ε) is between 0.8 and 1.2, which can be approximately considered as equal to 1. The natural frequencies of vibration of the front and rear parts of the vehicle body are represented by natural frequencies n_1 and n_2. the lower the vertical natural frequency of the vehicle, the better the damping effect of the suspension system, which leads to increased passenger comfort [11]. The respective natural frequencies of the front and rear parts of the vehicle body can be expressed by Equation (1).

$$n_1 = \sqrt{\frac{k_{s1}}{m_1}}\,;\, n_2 = \sqrt{\frac{k_{s2}}{m_2}} \tag{1}$$

The curb weight of the sightseeing vehicle is 1100 kg, comprising a sprung mass of 970 kg and an unsprung mass of 130 kg. Assuming each passenger weighs 60 kg, the total weight of eight fully seated passengers is 480 kg. Consequently, the sprung mass at this time is 1450 kg. Given that the axle load distribution ratio of the front axle is 60%, we can calculate the unsprung (m_1) and sprung masses (m_2) accordingly.

$$m_1 = 130/4 = 32.5\text{kg}$$

$$m_2 = (1450 \times 60\%)/2 = 435\text{kg}$$

In the design of vehicle suspension systems, considering the human body's sensitivity to vibration is crucial. According to the research by the International Organization for Standardization (ISO 2631-1:1997), the human body is more comfortable to vertical vibrations in the 1 – 1.5 Hz frequency range, and higher vibration frequencies can cause discomfort. Therefore, suspension systems are typically designed to keep the natural frequency of the vehicle body within the 1–1.5 Hz range to avoid the most sensitive frequency zone and enhance ride comfort. Based on this, assuming a natural frequency of n_1 = 1.0 Hz, the suspension stiffness can be further calculated to ensure the system meets comfort requirements. The stiffness of the front suspension can be determined using Equation (1):

$$k_{s1} = m_1 (2\pi n_1)^2 = 435 \times \left(2 \times 3.14 \times 1.0\right)^2 = 17155.7\text{N/m}$$

2.1. Damping Coefficient of Shock Absorber

In the suspension system, the stiffness of the elastic component is an important parameter for designing the damping performance of the suspension [12]. The flat value$\psi$of ψ_Y and ψ_s is chosen first. For suspension without friction elastic elements, it is common to take the value of $\psi = 0.25$~0.35; for suspension with elastic elements with internal friction, $\psi$is taken smaller to avoid suspension collision with the frame when preventing it, and $\psi_Y = 0.5\psi_s$.

Taking $\psi = 0.3$, the calculation result: $\psi_s = 0.4$ and $\psi_Y = 0.2$.

The damping coefficient of the shock absorber is determined by

$$\delta = 2\psi\sqrt{k_{s1} m_s}$$

$$\omega = \sqrt{k_{s1}/m_s}$$

$$\delta = 2\psi m_s \omega$$

The damping coefficient of shock absorber (δ) should be determined based on their specific layout characteristics. the damping coefficient is:

$$\delta = \frac{2\psi m_s \omega}{cos^2\alpha} \tag{2}$$

It is known that $\psi = 0.3$; $m_s = 435$kg; $\alpha = 30°$; $k_{s1} = 17155.7$N/m

Therefore, the damping coefficient of the shock absorber obtained by substituting the data is:

$$\delta = 2\psi m_s \omega / cos^2\alpha = 2\psi\sqrt{m_s c}\,/cos^2\alpha = 2165.5\text{N}\cdot\text{s/m}$$

2.2. Establishment of Kinematic Equations

The selection of state variables, road inputs, and output variables are *X*, *u*, and *Y* respectively:

$$X = \begin{bmatrix} \dot{Z}_2 & Z_2 & \dot{Z}_1 & Z_1 \end{bmatrix}^T$$

$$u = \begin{bmatrix} Z_g \end{bmatrix}$$

$$Y = \begin{bmatrix} \ddot{Z}_2 (Z_2 - Z_1) k_w (Z_1 - Z_g) \end{bmatrix}^T$$

Model assumptions: (1) Do not consider roll and pitch degrees of freedom; (2) The components of sprung loaded or unsprung loaded mass are rigidly connected; (3) The tire stiffness is a linear constant and always maintains contact with the road surface during motion. Based on the above assumptions, the suspension system can be described by the following differential equations [13]

$$m_1\ddot{Z}_1 - \delta\left(\dot{Z}_2 - \dot{Z}_1\right) - k_s\left(Z_2 - Z_1\right) + k_w\left(Z_1 - Z_g\right) = 0 \tag{3}$$

$$m_2\ddot{Z}_2 + \delta\left(\dot{Z}_2 - \dot{Z}_1\right) + k_s\left(Z_2 - Z_1\right) = 0 \tag{4}$$

In the formula: $\dot{Z}_2$: Sprung Mass Vertical Velocity (*m*/*s*); $\dot{Z}_1$: Unsprung Mass Vertical Velocity (*m*/*s*); $\ddot{Z}_2$: Body Acceleration (*m*/*s*^{2}); $Z_1 - Z_2$:Suspension Deflection (*m*); $k_w(Z_1 - Z_g)$: Dynamic Tire Load (*N*).

The solution to the dynamic Equations (3) and (4) is obtained as follows:

$$\ddot{Z}_2 = -\frac{\delta}{m_2}\dot{Z}_2 - \frac{\delta}{m_2}Z_2 + \frac{\delta}{m_2}\dot{Z}_1 + \frac{k_s}{m_2}Z_1$$

$$\ddot{Z}_1 = \frac{\delta}{m_1}\dot{Z}_2 + \frac{k_s}{m_1}Z_2 - \frac{\delta}{m_1}\dot{Z}_1 - \frac{\left(k_s + k_w\right)}{m_1}Z_1 + \frac{k_w}{m_1}Z_g$$

Subsequently, the state equation is derived as:

$$\begin{cases} \dot{X} = AX + BU \\ Y = CX + DU \end{cases}$$

In the formula:

$$A=\begin{bmatrix} -\dfrac{\delta}{m_2} & -\dfrac{k_s}{m_2} & \dfrac{\delta}{m_2} & \dfrac{k_s}{m_2} \\ 1 & 0 & 0 & 0 \\ \dfrac{\delta}{m_1} & \dfrac{k_s}{m_1} & -\dfrac{\delta}{m_1} & -\dfrac{\left(k_w+k_s\right)}{m_1} \\ 0 & 0 & 1 & 0 \end{bmatrix}$$

$$B=\begin{bmatrix} 0 & 0 & \dfrac{k_w}{m_1} & 0 \end{bmatrix}^T$$

$$C=\begin{bmatrix} -\dfrac{\delta}{m_2} & -\dfrac{k_s}{m_2} & \dfrac{\delta}{m_2} & \dfrac{k_s}{m_2} \\ 0 & 1 & 0 & -1 \\ 0 & 0 & 0 & k_w \end{bmatrix}$$

$$D=\begin{bmatrix} 0 & 0 & -k_w \end{bmatrix}^T$$

2.3. Road Incentive Modeling

The current methods for time-domain modeling of roads at home and abroad mainly include harmonic superposition method, time series modeling method, inverse Fourier transform method, and filtered white noise method [14]. Among them, the filtered white noise method is currently the most widely used road roughness simulation method. This article uses this method to simulate road roughness. This article uses simple pulse signals combined with filtered white noise road roughness signals as random road excitation. The time-domain model for filtering white noise road roughness is:

$$\dot{z}_0(t)=-2\pi n_1 u z_0(t)+2\pi n_0\sqrt{G_q\left(n_0\right)u}\ \omega(t)$$

Here $n_1=0.01m^{-1}$

The simple pulse signal can be understood as a convex hull road surface within 1.0~1.5 s. Referring to ISO standards, road roughness is divided into 8 levels, represented by A~H (ISO 8608:2016), where Grade A represents extremely smooth roads and Grade H represents very rough surfaces. In this study, B-grade pavement is used. And the value obtained from the table for road roughness coefficient ($G_q(n_0)$) is 0.000064. Specifically, Grade B represents relatively smooth roads, typically used for comfort testing or design standards for passenger cars.

MATLAB/Simulink is used as the platform to build the random pavement simulation excitation suspension model, as shown in Figure 2. The stochastic pavement excitation model includes a filtered white noise generator, two gain modules K_1 and K_2, an integrator and an oscillator. The gain $K_1=2\pi n_0\sqrt{G_q(n_0)u}$, $K_2=2\pi n_1 u$.

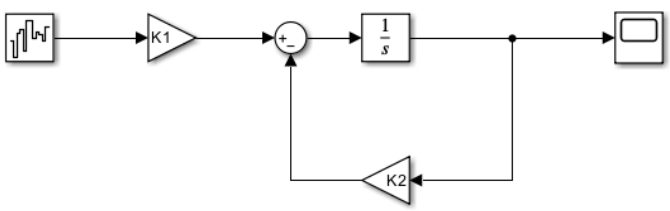

Figure 2. Random road excitation model.

When setting two gain modules, the value of $G_q\left(n_0\right)$ should correspond to the corresponding road surface unevenness coefficient, and u represents the simulated vehicle speed. The parameters of the bandlimited white noise module include noise power, sampling time, and seed, which play a decisive role in the output results of the simulation. Due to the MATLAB/Simulink platform providing a bilateral power spectrum. In the simulation model, what is needed is a bandlimited white noise with a unilateral power spectrum of 1. Therefore, the noise power needs to be set to 0.5 to ensure that the output power of the bandlimited white noise is a certain value. The sampling time of the limited white noise module is set to 1/10 u, and the unit of vehicle speed u is m/s. This sampling frequency ensures that the simulated vehicle speed is, and the distance traveled within 1 s includes 10 u sampling points [13] (i.e., the sampling time is set to 0.005). The seed value in the bandlimited white noise module does not need to be changed, just keep it as default. This article establishes a B-level random road excitation model in Simulink, with a simulated vehicle speed of 20 m/s. The obtained B-level random simulated road roughness is shown in Figure 3.

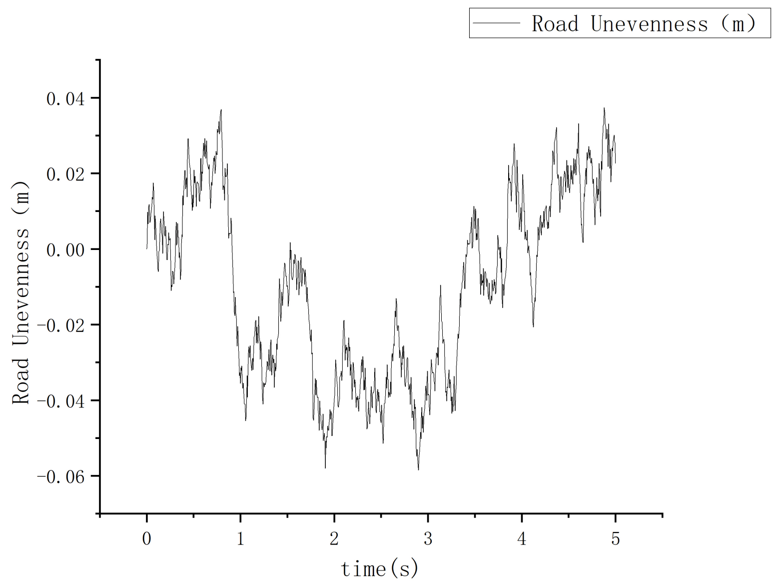

Figure 3. B-grade road excitation.

Using Simulink's state equation to establish a vehicle dynamics model, combined with a random road excitation model for simulation, the vibration simulation diagram under B-level road excitation is shown in Figures 4 and 5.

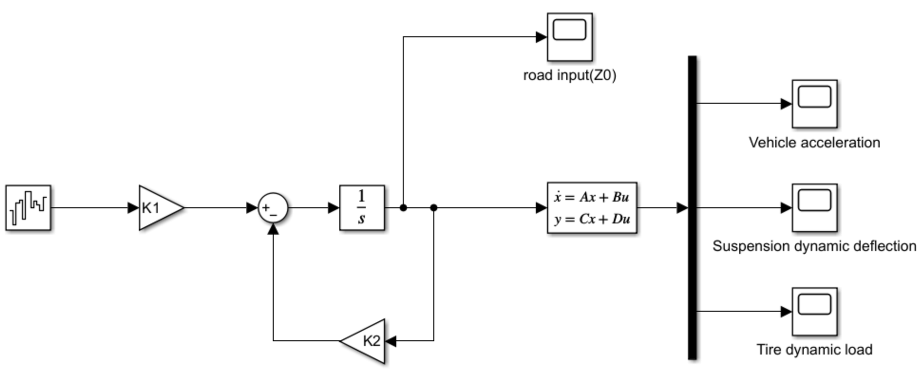

Figure 4. Vibration simulation diagram under B-grade road excitation.

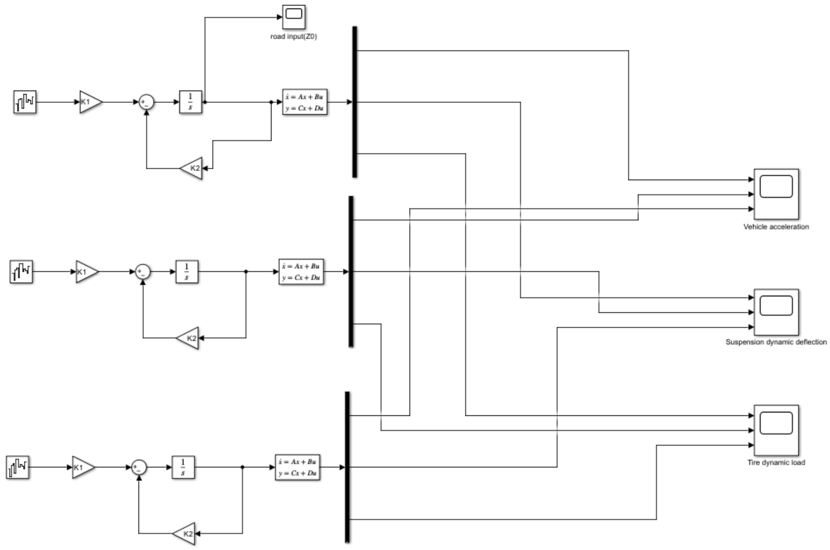

Figure 5. Comparison simulation graph of different suspension stiffness.

3. Results and Discussion

Suspension vibration is influenced by various factors, and the following are some of the main factors [15]: road conditions, driving speed, vehicle mass, suspension stiffness, tire characteristics, driver operation, among which suspension stiffness is a vital factor affecting suspension vibration. Next, this study will analyze the impact of different suspension stiffness settings on the suspension vibration characteristics of the sightseeing vehicle.

Taking the 1/4 front MacPherson suspension as an example for simulation analysis, the relevant parameters are: non-sprung mass of 32.5 kg, sprung mass of 435 kg, tire stiffness of 192, 000 N/m, and damper damping coefficient of 2165.5 N·s/m. Once the parameter settings are completed, simulation time-domain analysis can be conducted. The simulation time is set to 5 s, and the suspension stiffness values are 17,155.7 N/m, 18,500 N/m, and 21,000 N/m. The vehicle acceleration, suspension dynamic deflection, and tire dynamic load of this design can be obtained through vibration simulation under B-level road excitation. To achieve the above simulation, program code is written in MATLAB scripts.

3.1. Vibration Performance Simulation Results

3.1.1. Comparison of Vehicle Vertical Acceleration

The vertical acceleration of the vehicle body is one of the main indicators to describe the smoothness of car driving. Vertical acceleration describes the dynamic motion of the vehicle in the vertical direction, reflecting how much the vehicle bounces up and down. When driving on uneven roads or encountering sudden stops, the vertical acceleration of the vehicle body can spike, increasing the discomfort felt by passengers. Higher vertical acceleration means the vehicle will have more pronounced upward and downward movements when encountering bumps, which can cause discomfort to passengers, such as headaches and motion sickness. Conversely, lower vertical acceleration allows the vehicle to travel more smoothly, reducing passenger discomfort and enhancing riding comfort. Therefore, reducing the vertical acceleration of the vehicle body effectively minimizes vehicle vibration, thereby improving smoothness in driving and passenger comfort. The specific waveform of the vehicle body's vertical acceleration is shown in Figure 6. For ease of analysis, the simulation data are analyzed by taking the absolute values, and then performing statistical analysis on the mean, standard deviation, and maximum value. The same method is used for all the following statistical data, so further details are omitted.

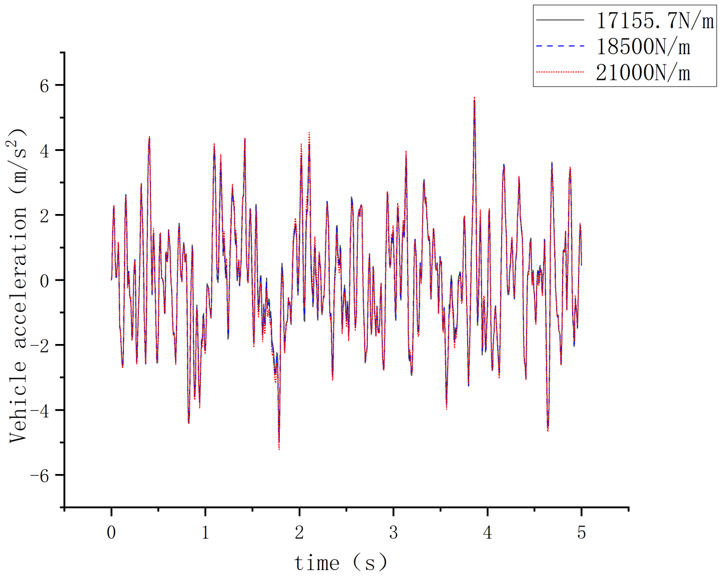

Figure 6. Comparison chart of vehicle vertical acceleration.

To enhance the visual representation of the information, we performed numerical analysis on the waveform to obtain the data presented in Table 3.

Table 3. The vehicle vertical acceleration data under different stiffness.

Stiffness	17,155.7 N/m	18,500 N/m	21,000 N/m
Average	1.344	1.362	1.398
std	1.015	1.027	1.051
max	5.489	5.533	5.643

Suspension stiffness affects vehicle comfort and handling performance [16]. When the suspension stiffness is low, the suspension system is relatively soft and can absorb more road impacts and vibrations. Therefore, at a stiffness of 17, 155.7 N/m, the vertical acceleration of the vehicle body may be relatively small, resulting in better ride comfort. However, overly soft suspension may cause significant body roll when driving at high speeds or during turns, affecting handling stability.

As the suspension stiffness increases, the suspension system provides better balance, absorbing some road impacts while maintaining a certain level of handling stability. Consequently, the vertical acceleration of the vehicle body may be at a moderate level, ensuring both ride comfort and without sacrificing handling performance excessively. When the suspension stiffness reaches 21,000 N/m, the suspension system is stiff, resulting in poor adaptation to road impacts. This may lead to significant vertical acceleration of the vehicle body when encountering rough road surfaces, impacting ride comfort.

In practical applications, vehicle engineers employ various means to reduce the vertical acceleration of the vehicle body, such as optimizing suspension system design, adjusting spring stiffness and damping coefficients, and utilizing advanced suspension system technology. These measures aim to decrease vehicle vibration, enhance ride comfort, and improve handling stability, providing users with a better driving experience.

By comparing different damping parameters 2000, 2165.5, and 2300 N · s/mwith suspension damping as a variable, the conclusion can be drawn. The vertical acceleration of the vehicle body tends to increase with the increase of suspension damping. Detailed image and numerical table can be found in Figure 7 and Table 4.

According to the statistical data in the Table 4, as the suspension damping increases, both the peak value and the average value of vehicle vertical acceleration increase.

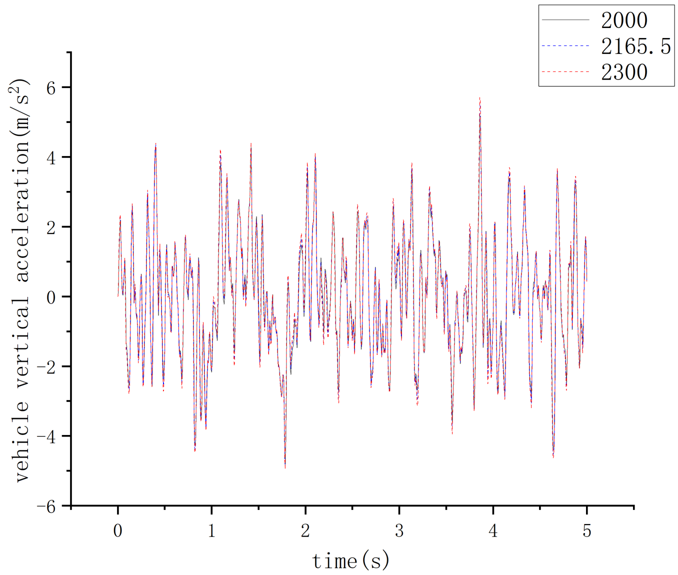

Figure 7. Comparison diagram of vehicle vertical acceleration based on suspension damping.

Table 4. Vehicle vertical acceleration data based on suspension damping.

Damping	2000 N·s/m	2165.5 N·s/m	2300 N·s/m
mean	1.310	1.344	1.373
std	0.980	1.015	1.042
max	5.194	5.490	5.710

3.1.2. Comparison of Suspension Dynamic Deflection

The dynamic deflection of the suspension refers to the vertical displacement of the wheel center relative to the frame (or body) when the suspension is compressed from the fully loaded static equilibrium position to the maximum allowable deformation of the structure (usually referring to the compression of the buffer block to 1/2 or 2/3 of its free height). Generally speaking, the suspension deflection of a sightseeing car should be within a safe range to ensure passenger comfort and safety. If the suspension deflection is too large, it may cause passengers to feel uncomfortable or panic, and may even pose a threat to their health and safety.

In the case of a suspension stiffness of 21,000 N/m, the dynamic deflection is relatively high, which means that the suspension system allows greater displacement to cope with the unevenness of the road surface. This configuration enables the vehicle to better absorb shocks when encountering potholes, bumps, or uneven roads, thereby reducing the vibrations and swaying of the body, and enhancing ride comfort. However, excessive dynamic deflection might also lead to side tilting and swaying when the vehicle is traveling at high speeds, affecting handling stability. At 17,155.7 N/m, the dynamic deflection is smaller, and the suspension system is relatively stiff, making it less adaptable to uneven roads. In this scenario, the vehicle may experience greater vibrations and swaying when encountering bumpy roads, impacting ride comfort. However, a smaller dynamic deflection usually indicates that the suspension system is more stable, providing better handling and response speed [17]. The specific changes in suspension dynamic deflection are shown in Figure 8 and Table 5. Actual comfort and operational stability should be reasonably judged by referring to other factors.

Table 5. The suspension dynamic deflection data under different stiffness.

Stiffness	17,155.7 N/m	18,500 N/m	21,000 N/m
mean	0.0117	0.0119	0.0122
std	0.0096	0.0097	0.0098
max	0.04120	0.0436	0.0457

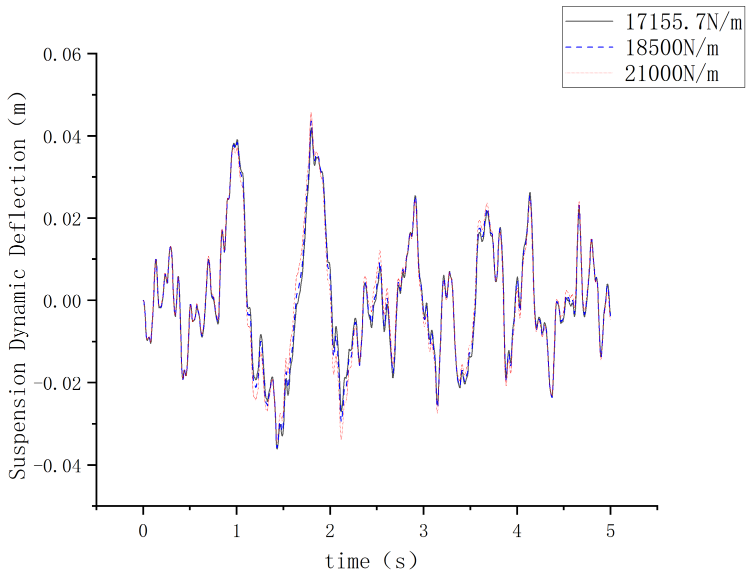

Figure 8. Comparison of suspension dynamic deflection.

In general scenarios, the greater the stiffness, the harder the suspension is, so the suspension deflection should be less. In this study, the observation is opposite.

To verify if other B-class random road surfaces exhibit the same pattern, we conducted observations by altering the random factor of the random road surface. Another B-level random road surface is obtained, with the specific waveform shown in Figure 9.

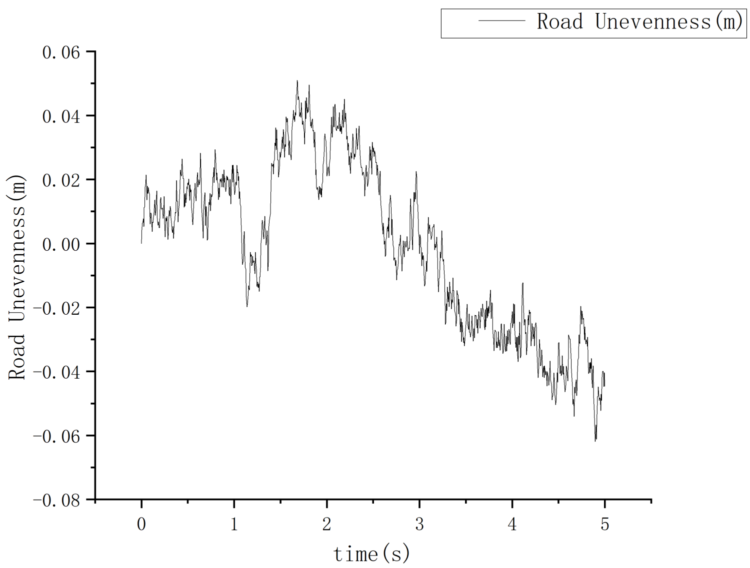

Figure 9. B-grade road excitation.

Under this random road excitation, the results are the same. See the waveform and data in Figure 10 and Table 6 for details.

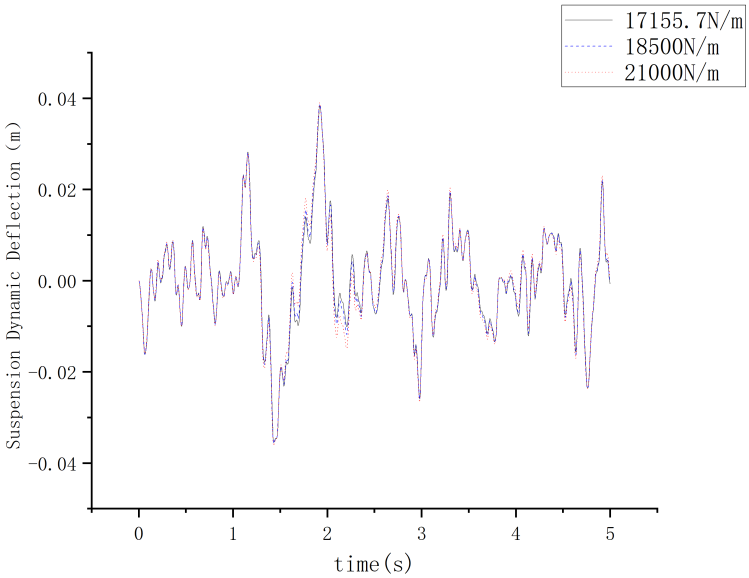

Figure 10. Comparison of suspension dynamic deflection.

Table 6. The suspension dynamic deflection data under different stiffness.

Stiffness	17,155.7 N/m	18,500 N/m	21,000 N/m
mean	0.0080	0.0081	0.0084
std	0.0075	0.0075	0.0076
max	0.0383	0.0388	0.0390

According to the statistical data in Table 6, as the suspension stiffness increases, both the peak value and the average value of suspension dynamic deflection increase.

For vehicles with significant load variations, such as heavy trucks, even if the suspension system is designed with high stiffness, increased external forces during full or overloaded conditions can lead to greater suspension deformation [9]. In such cases, the suspension system exhibits deformation behavior that is inconsistent with its stiffness when unloaded. The same result is observed when applied to passenger vehicles such as sightseeing buses. When the sprung mass of the sightseeing vehicle is set to a lower value, such as 35 kg, and statistical analysis is conducted, the results align with common understanding: greater stiffness leads to a harder suspension and less suspension deformation. Detailed numerical table can be found in Table 7.

Table 7. The suspension dynamic deflection data under different stiffness.

Stiffness	17,155.7 N/m	18,500 N/m	21,000 N/m
mean	0.0047	0.0047	0.0047
std	0.0036	0.0036	0.0036
max	0.0198	0.0197	0.0196

To ensure the safety of the sightseeing bus and the comfort of passengers, it should be regularly inspected and maintained to ensure that it is in good working condition.

By observing the waveform and comparing the data, it can be seen that as the suspension stiffness increases, the average value of suspension dynamic deflection remains relatively constant, but the peak value decreases.

According to the statistical data in Table 8 and image in Figure 11, as the suspension damping increases, both the peak value and the average value of suspension dynamic deflection decrease.

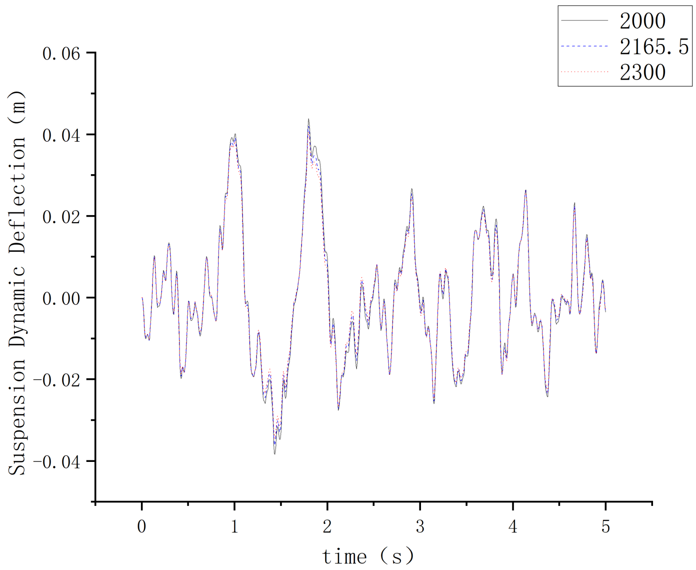

Figure 11. Comparison of suspension dynamic deflection based on suspension damping.

Table 8. The suspension dynamic deflection data under different damping.

Damping	2000 N·s/m	2165.5 N·s/m	2300 N·s/m
mean	0.0122	0.0117	0.0114
std	0.0100	0.0096	0.0093
max	0.0439	0.0420	0.0410

3.1.3. Tire Dynamic Load Comparison

Tire dynamic load refers to the change in downward pressure exerted by a tire on the ground during driving, which is the load change caused by the displacement of the tire relative to its static equilibrium state. This load change will further affect the contact force between the tire and the ground, thereby affecting the driving performance of the vehicle.

In this simulation process, it shows an increasing trend with the increase of suspension stiffness. The specific waveform is shown in Figure 12. When the suspension stiffness is at 17,155.7 N/m, the suspension system is softer, which allows it to better adapt to uneven road surfaces and reduce the impact on the tires. In this case, the contact force between the tire and the road might be more even, helping to reduce tire wear. As stiffness increases, the contact force between the tire and the road fluctuates within a certain range, which may affect tire wear. When the suspension stiffness reaches 21,000 N/m, the tires are subjected to greater impact forces, especially when encountering potholes or raised surfaces. This might lead to increased localized wear on the tires, and even affect tire lifespan.

The tire dynamic load of a sightseeing bus is related to multiple factors such as tire design, materials, air pressure, speed, road conditions, as well as the weight and load of the vehicle itself. For vehicles used in venues such as sightseeing buses, due to their relatively low speed but potentially high load-bearing capacity, tires need to have good strength, load-bearing capacity, and wear resistance. At the same time, the adhesion performance between the tire and the ground is also important to ensure sufficient grip during acceleration, braking, and steering. When the sightseeing bus travels on uneven roads or encounters unexpected situations, the tires will be affected by dynamic loads, namely tire dynamic loads. If the tire dynamic load is too large, it may cause poor contact between the tire and the ground, increase vehicle vibration and impact, and affect passenger comfort and vehicle safety. Therefore, when designing and selecting tires for sightseeing vehicles, it is necessary to comprehensively consider the static and dynamic load capacity of the tires, as well as their performance under various road conditions.

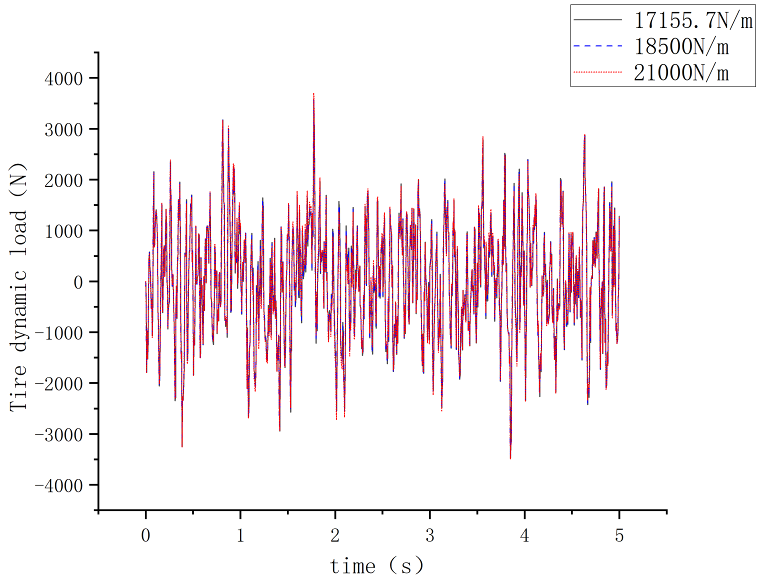

Figure 12. Tire dynamic load waveform diagram.

By observing the waveform and comparing the data in Table 9, it can be seen that as the suspension stiffness increases, the average value of dynamic load on the tire slightly increases, but the peak value increases significantly.

Table 9. The Tire dynamic load data under different stiffness.

Stiffness	17,155.7 N/m	18,500 N/m	21,000 N/m
mean	878.320	880.730	886.027
std	636.117	637.847	642.170
max	3562.990	3616.690	3704.999

According to the statistical data in Table 10, as the suspension damping increases, both the peak value and the average value of tire dynamic load decrease slowly. Please refer to Figure 13 for the specific Tire dynamic load waveform diagram.

Table 10. Tire dynamic load data under different damping.

Damping	2000 N·s/m	2165.5 N·s/m	2300 N·s/m
mean	882.475	878.294	876.663
std	635.688	636.099	637.969
max	3566.612	3562.986	3561.473

The above rules are summarized in Table 11, where the suspension stiffness and suspension deflection are increased by default.

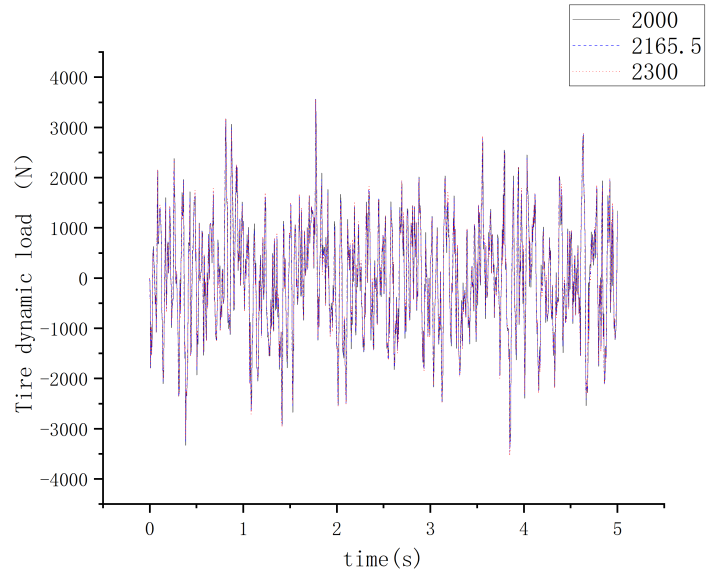

Figure 13. Tire dynamic load waveform diagram based on suspension damping.

Table 11. Simulation Summary.

	Suspension Stiffness	Suspension Damping
vehicle vertical acceleration	increase	increase
Suspension Dynamic Deflection	increase	decrease
Tire dynamic load	increase	decrease

Because the vertical acceleration of the vehicle body reflects the vertical vibration experienced by the vehicle during driving, a smaller vertical acceleration means that the vehicle can better isolate the impact of uneven road conditions, which is more likely to affect the comfort and stability of the ride. Excessive dynamic deflection of the suspension may cause the suspension system to hit the limit block, reducing the service life of the shock absorber. High dynamic tire loads not only reduce driving stability, but more importantly, they can place additional strain on the vehicle's suspension system, braking system, and other components, causing increased wear and tear on these components, which in turn affects the overall performance and longevity of the vehicle. Therefore, if you want to pursue comfort and stability in the sightseeing car ride, you can reduce the vertical acceleration of the body by using a lower suspension stiffness and damping. If the service life of the vehicle is pursued, a lower suspension stiffness and higher suspension damping can be adopted. To verify this hypothesis, both suspension stiffness and deflection are set as variables, and the simulation results are observed.

The subsequent simulation is based on Table 12.

Table 12. Simulation Validation Control.

Reference	Control Group 1	Control Group 2
ks = 17,155.7	ks2 = 16,000	ks3 = 15,000
c1 = 2165.5	c2 = 1900	c3 = 2300

In the simulation data reference and Control Group 1, by reducing the suspension stiffness and damping, a significant decrease in both the average value and peak value of vehicle vertical acceleration was observed, confirming the first hypothesis: If you want to pursue comfort and stability in the sightseeing car ride, you can reduce the vertical acceleration of the body by using a lower suspension stiffness and damping. Detailed image and numerical table can be found in Figure 14 and Table 13.

Table 13. Vehicle vertical acceleration.

	Reference	Control_Group_1	Control_Group_2
mean	1.275	1.199	1.295
std	0.999	0.935	1.004
max	5.325	5.074	5.308

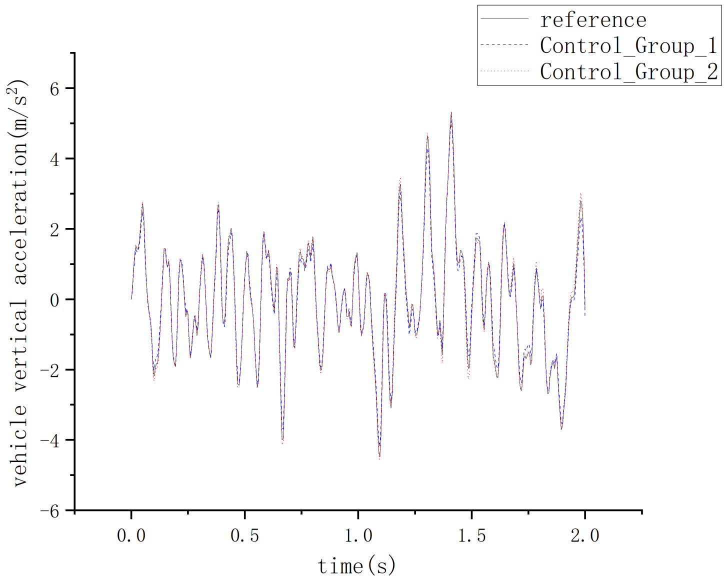

Figure 14. Vehicle vertical acceleration.

In the simulation data reference and Control Group 2, by reducing the suspension stiffness and increasing the suspension damping, it was found that both the average value and peak value of suspension dynamic deflection decreased, confirming the second hypothesis: If the service life of the vehicle is pursued, a lower suspension stiffness and higher suspension damping can be adopted. Detailed image and numerical table can be found in Figure 15 and Table 14.

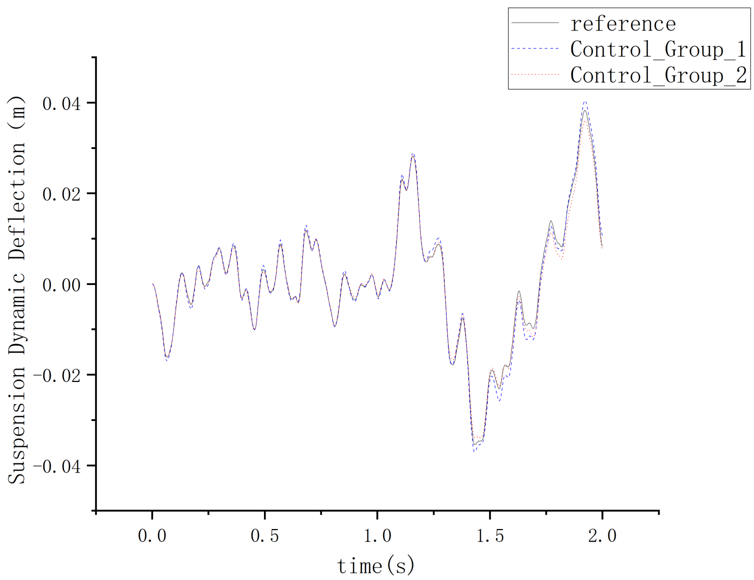

Figure 15. Suspension dynamic deflection.

Table 14. Suspension dynamic deflection.

	Reference	Control_Group_1	Control_Group_2
mean	0.0099	0.0105	0.0096
std	0.0096	0.0100	0.0092
max	0.0383	0.0404	0.0360

Although the peak value of tire dynamic load has slightly increased, there is a decrease in the average value. Considering the influence of suspension deflection, the second hypothesis can still be validated. Detailed image and numerical table can be found in Figure 16 and Table 15.

Table 15. Tire dynamic load.

	Reference	Control_Group_1	Control_Group_2
mean	871.173	881.009	869.621
std	632.801	628.381	631.928
max	3178.128	3063.184	3190.786

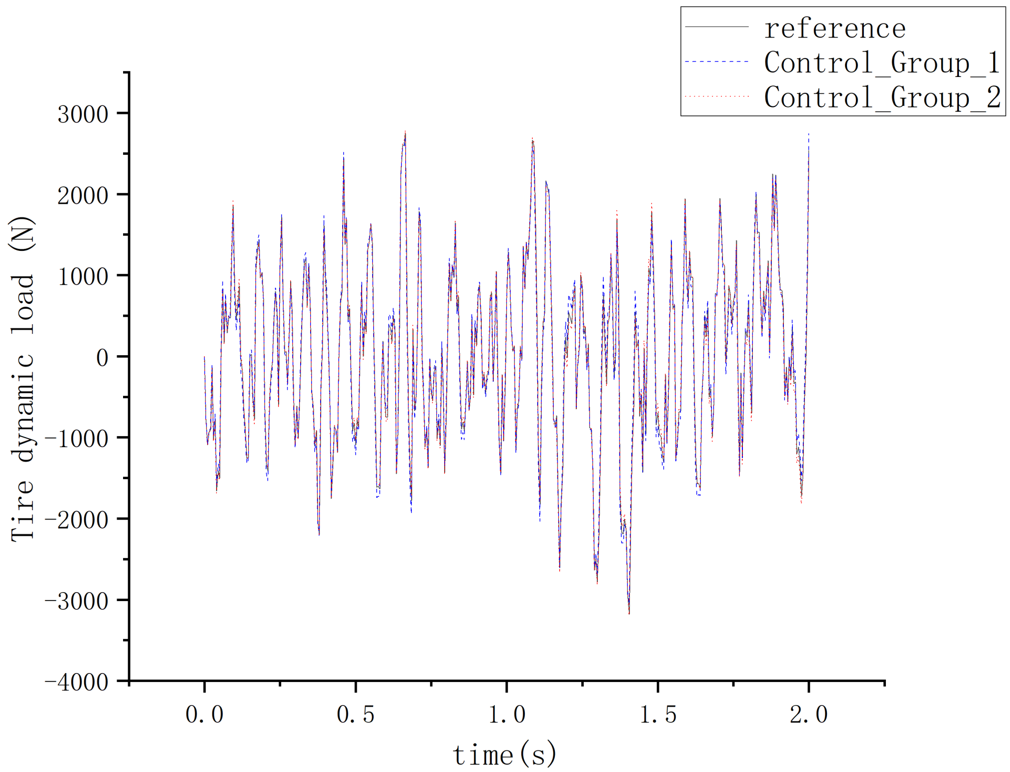

Figure 16. Tire dynamic load.

4. Conclusion

In this study, a dynamic model of the suspension system is established by using MATLAB/Simulink software, and a simulation analysis of its vibrational characteristics is conducted. The key parameters including vehicle body acceleration, suspension deflection, and tire dynamic load are obtained, providing a solid basis for evaluating the suspension performance. By comparing the simulation results under different stiffness and damping parameters, we can conclude that while a certain level of suspension stiffness is necessary for the overall ride comfort of the vehicle, it is not always the case that higher stiffness is better. Analysis of the simulated waveforms indicates that excessively high suspension stiffness may lead to reduced ride comfort and lower passenger comfort during vehicle operation. Therefore, if you want to pursue comfort and stability in the sightseeing car ride, you can reduce the vertical acceleration of the body by using a lower suspension stiffness and damping. If the service life of the vehicle is pursued, a lower suspension stiffness and higher suspension damping can be adopted.

Author Contributions: D.L.: methodology, software, visualization; L.R.: data curation; N.M.: writing—original draft preparation, investigation; Y.S.: writing—reviewing and editing; R.L.: supervision; J.Y.: software, validation. All authors have read and agreed to the published version of the manuscript.

Funding: This work was supported by the Shandong Provincial Natural Science Foundation of China (No. ZR2021QB137, ZR2021QA067 and ZR2022ME082), the National Natural Science Foundation of China (No. 12002142), the Youth Entrepreneurship Technology Support Program for Higher Education Institutions of Shandong Province (No. 2023KJ215), the Shandong Provincial Science and Technology Improvement Plan Project (No.2023TSGC0426) and the Scientific Research of Linyi University (Nos.Z620622003 and 2021PTXM001).

Institutional Review Board Statement: Not applicable.

Informed Consent Statement: Not applicable.

Data Availability: Statement: The data that support the findings of this study are available at [https://detail.1688.com/offer/676740586294. html&scm=1007.45324.363797.0&pvid=67677cc5-7b22-45b9-974d-ba5049cd36a0? spm= a262cb.19918180.ljxo5qvc.4.27421a5aP8b2IV&file=676740586294.html&scm=1007.45324.363797.0&pvid=67677cc5-7b22-45b9-974d-ba5049cd36a0] (accessed on 14 March 2024). These data were derived from the following resources available in the public domain: [https://cbu01.alicdn.com/img/ibank/O1CN01vitayR1ht1JJGhz3e_!!2213235674334-0-cib.jpg?__r__=1655113378789] (accessed on 14 March 2024).

Conflicts of Interest: No potential conflict of interest was reported by the authors.

References

1. Xu, X.; Zhou, K.; Zou, N.; Jiang, H.; Cui, X. Multi-objective Optimization and Experimental Investigation of Quarter Car Suspension System. *Int. J. Dyn. Control* **2023**, *12*, 1222–1238.
2. Lin, D.T.; Lei, Y.L. Analysis of Safety Hazards in Tourist Car Occupant Seating. *China Spec. Equip. Saf.* **2022**, *38*, 72–76+80.
3. Xu, X.; Zhou, K.; Zou, N.; Jiang, H.; Cui, X. Hierarchical Control of Ride Height System for Electronically Controlled Air Suspension Based on Variable Structure and Fuzzy Control Theory. *Chin. J. Mech. Eng.* **2015**, *28*, 945–953.
4. Popescu, F.; Chivu, R.M.; Uzuneanu, K.; Ion, I. Design and Finite Element Analysis of a Lower Arm Using CATIA V5. *IOP Conf. Ser. Mater. Sci. Eng.* **2022**, 1262, 012070.
5. Balena, M.; Mantriota, G.; Reina, G. Dynamic Handling Characterization and Set-Up Optimization for a Formula SAE Race Car via Multi-Body Simulation. *Machines* **2021**, *9*, 126–126.
6. Karthikeyan, R.; Rajkumar, S.; Bensingh, R.J.; Kader, M.A.; Nayak, S.K. Finite Element Analysis of Elastomer Used in Automotive Suspension Systems. *J. Elastomers* **2020**, *52*, 521–536.
7. Sadegh, Y.; Abolfazl, K.; Christian, C. Robust Design of Multi-Body Model of Steering Mechanism Based on Uncertainties of Suspension Parameters. *J. Braz. Soc. Mech. Sci. Eng.* **2023**, 45, 482.
8. Dong, M. Modeling and Simulation Analysis of Different Suspension Systems for Vehicles. *Automot. Pract. Technol.* **2022**, *47*, 123–126.
9. Rajamani, R. *Vehicle Dynamics and Control*; Springer: New York, NY, USA, 2012.
10. Rusu, I.C.M.; Suciu, C.; Mihai, I. Analysis of Passive vs. *Semi-Active Quarter Car Suspension Model. Adv. Top. Optoelectron. Microelectron. Nanotechnol. X* **2020**, *11718*, 428–433.
11. Mitschke, M.; Wallentowitz, H. *Dynamik der Kraftfahrzeuge*, 4th ed.; Springer: Berlin, Germany, 2004.
12. Jiang, Q.K.; Wu, X.J. Simulation Analysis of Main Parameter Matching for Automotive Suspension. *Agric. Equip. Veh. Eng.* **2022**, *60*, 125–128+133.
13. Wei, S.S. Simulation Analysis of Suspension Performance with Two Degrees of Freedom under Random Road Excitation. *Agric. Equip. Veh. Eng.* **2023**, *61*, 136–139.
14. Yin, J.; Chen, X.; Wu L. Time-domain Simulation Method of Filtered White Noise Road Surface and Suspension Performance Simulation. *J. Tongji Univ.* **2017**, *45*, 398–407.
15. Tandel, A.; Deshpande, A.R.; Deshmukh, S.P.; Jagtap, K.R. Modeling, analysis and PID controller implementation on double wishbone suspension using SimMechanics and Simulink. *Proc. Eng.* **2014**, *97*, 1274–1281.
16. Bao, Z.; Hongnan, W.; Zhi L.; Tangyun Z. Stiffness design and mechanical performance analysis of transverse leaf spring suspension. *J. Mech. Sci. Technol.* **2023**, *37*, 1339–1348.
17. Yang, F.; Zhao, L.; Yu, Y.; Zhou, C. Matching, stability, and vibration analysis of nonlinear suspension system for truck cabs. *Shock Vib*. **2019**, *2019*, 1490980.